ELSEVIER

Biochimica et Biophysica Acta 1565 (2002) 97–106

BIOCHIMICA ET BIOPHYSICA ACTA
BBA

www.bba-direct.com

Residue-specific millisecond to microsecond fluctuations in bacteriorhodopsin induced by disrupted or disorganized two-dimensional crystalline lattice, through modified lipid–helix and helix–helix interactions, as revealed by ^{13}C NMR

Hazime Saitô *, Takahiro Tsuchida, Keizi Ogawa, Tadashi Arakawa, Satoru Yamaguchi, Satoru Tuzi

Department of Life Science, Graduate School of Science, Himeji Institute of Technology, Harima Science Garden City, Kouto 3 chome, Kamigori, Hyogo 678-1297, Japan

Received 17 April 2002; received in revised form 2 July 2002; accepted 11 July 2002

Abstract

We have recorded ^{13}C NMR spectra of [3-^{13}C]-, [1-^{13}C]Ala-, and [1-^{13}C]Val-labeled bacteriorhodopsin (bR), W80L and W12L mutants and bacterio-opsin (bO) from retinal-deficient E1001 strain, in order to examine the possibility of their millisecond to microsecond local fluctuations with correlation time in the order of 10^{-4} to 10^{-5} s, induced or prevented by disruption or assembly of two-dimensional (2D) crystalline lattice, respectively, at ambient temperature. The presence of disrupted or disorganized 2D lattice for W12L, W80L and bO from E1001 strain was readily visualized by increased relative proportions of surrounding lipids per protein, together with their broadened ^{13}C NMR signals of transmembrane α-helices and loops in [3-^{13}C]Ala-labeled proteins, with reference to those of wild-type. In contrast, ^{13}C CP-MAS NMR spectra of [1-^{13}C]Ala- and Val-labeled these mutants were almost completely suppressed, owing to the presence of fluctuations with time scale of 10^{-4} s interfered with magic angle spinning. In particular, ^{13}C NMR signals of [1-^{13}C]Ala-labeled transmembrane α-helices of wild-type were almost completely suppressed at the interface between the surface and inner part (up to 8.7 Å deep from the surface) with reference to those of the similarly suppressed peaks by Mn^{2+}-induced accelerated spin–spin relaxation rate. Such fluctuation-induced suppression of ^{13}C NMR peaks from the interfacial regions, however, was less significant for [1-^{13}C]Val-labeled proteins, because fluctuation motions in Val residues with bulky side-chains at the C_α moiety were modified to those of longer correlation time (>10^{-4} s), if any, by residue-specific manner. To support this view, we found that such suppressed ^{13}C NMR signals of [1-^{13}C]Ala-labeled peaks in the wild-type were recovered for D85N and bO in which correlation times of fluctuations were shifted to the order of 10^{-5} s due to modified helix–helix interactions as previously pointed out [Biochemistry, 39 (2000) 14472; J. Biochem. (Tokyo) 127 (2000) 861].

Keywords: Bacteriorhodopsin; Membrane protein; ^{13}C NMR; Two-dimensional crystalline lattice; Lipid–helix interaction; Helix–helix interaction

1. Introduction

Many integral membrane proteins in the membrane environment are known to assemble into oligomeric complexes rather than monomers to form tertiary and quaternary structures necessary for biological signaling [1,2]. Such oligomeric complexes have been confirmed in view of the three-dimensional (3D) pictures of membrane proteins revealed either from two-dimensional (2D) or 3D crystals, including light-driven proton pump bacteriorhodopsin (bR) [3–7], chloride pump halorhodopsin [8,9], and phototaxis receptor sensory rhodopsin II [10–12], photosynthetic reaction center [13], light-harvesting complex [14,15], cytochrome *c* oxidase [16,17], potassium and mechanosensitive channels [18,19], etc. It is expected from these data that stabilization energies might be gained by this oligomerization process, although biological activity of reconstituted bR as proton pump, for instance, turned out to be native-like in spite of the monomeric form [20].

In particular, proton pump bR from *Halobacterium salinarum* assembles into naturally occurring two-dimen-

* Corresponding author. Fax: +81-791-58-0182.
E-mail address: saito@sci.himeji-tech.ac.jp (H. Saitô).

0005-2736/02/$ - see front matter © 2002 Elsevier Science B.V. All rights reserved.
PII: S0005-2736(02)00513-8

sional (2D) crystalline patches known as purple membrane (PM) in which its trimeric unit is hexagonally packed under physiological condition [21] and is active as light-driven proton pump to translocate protons from the inside to the outside of the cell [22]. The gained stabilization energy for the lattice formation in 2D crystals of bR was estimated as at least 5 kcal/mol as compared to the monomeric form [23], although greater stability of the constituent bR trimer is mainly by entropic factors [24]. Interestingly, 3D crystals of bR grown from the cubic phase is also arranged in the hexagonal packing with the same unit cell as that of native 2D crystal [25,26]. Nevertheless, tetrameric arrangement of chloride pump halorhodopsin in 2D crystal [8] is not retained in 3D crystal prepared from the cubic phase, but trimeric complex is formed instead [9]. In such arrangement of bR trimer, 10 lipid molecules per bR monomer, comprised of six to seven phospholipids, two to three sulfoglycolipids and one squalene fill the space between the proteins [27,28]. The presence of such endogeneous lipids is essential for the 2D crystalline array of bR when one attempts to regenerate it by incorporation into dimyristoylphosphatidylcholine (DMPC) bilayer [29]. In addition to such lipid–protein interactions to the lattice assembly, helix–helix interaction is also very important as manifested from its modification by removal of retinal from bR, because bacterio-opsin (bO) from retinal-deficient strain exhibited a low degree of hexagonal order [30–32]. This kind of picture has also been obtained by introduction of site-directed mutation at specific positions essential for such interactions as a very important determinant for purple membrane assembly [33–35].

Naturally, resulting conformational changes in the protein backbone have been recognized during the course of the lattice assembly when bR was regenerated by addition of retinal to bO prepared from either hydroxylamine-treated bR or retinal-deficient strain [25,36,37]. Accompanied dynamics as well as conformational changes are prerequisite to permit entry of retinal to bO to form bR, as conveniently examined by ^{13}C NMR [32], although no such data as to dynamic feature is available from the experimental means based on measurements at low temperature. Instead, ^{13}C NMR measurements of fully hydrated ^{13}C-labeled bR provide one excellent, non-perturbing means to be able to probe underlying local dynamic changes with correlation times of 10^{-4} to 10^{-5} s *at ambient temperature* [38,39]. Undoubtedly, the dynamic aspect of membrane proteins comprised of a very flexible and dynamically heterogeneous structure with local motional frequencies varying from the

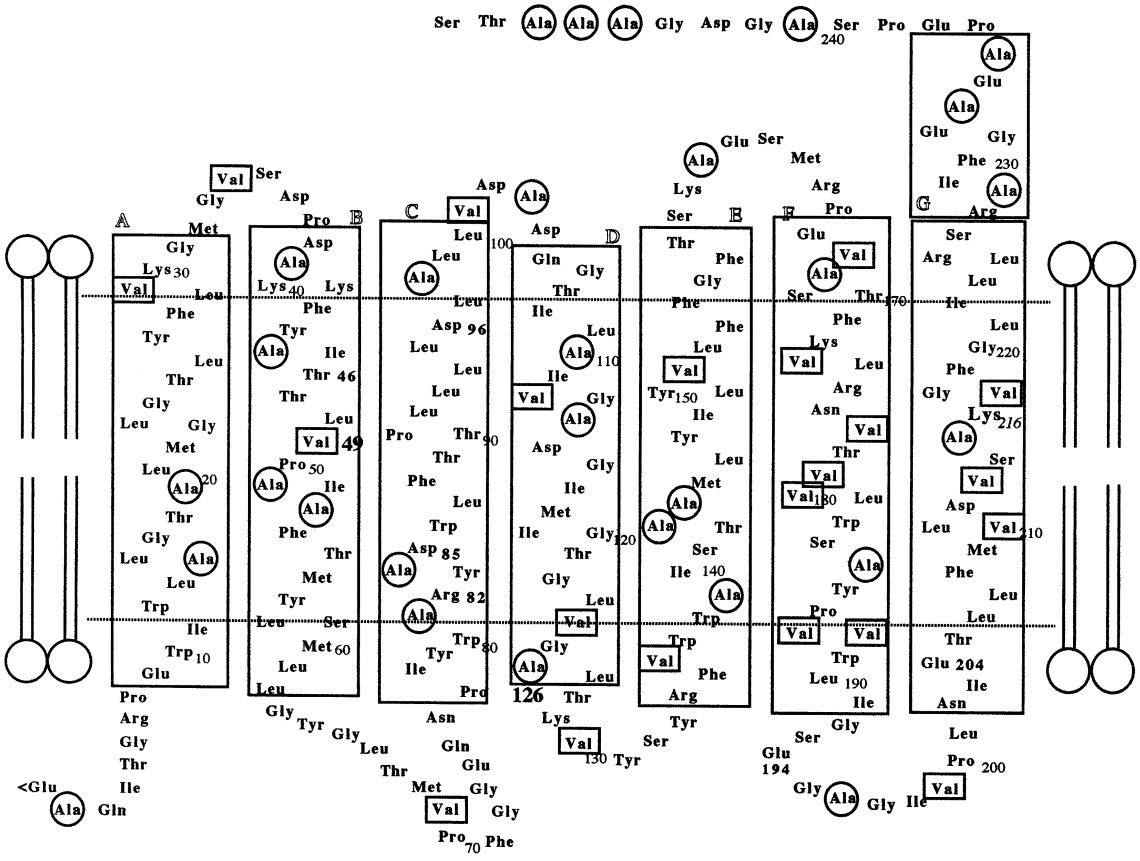

Fig. 1. Schematic representation of the secondary structure of bacteriorhodopsin. All Ala and Val residues labeled by [^{13}C]Ala- and [1-^{13}C]Val- are indicated by the circles and boxes, respectively. Horizontal lines were drawn to roughly indicate the boundary between interfacial and inner parts in the transmembrane α-helices based upon spectral changes as noted for Mn^{2+}-induced suppression of peaks for [3-^{13}C]Ala-bR [52] and [1-^{13}C]Pro-bR (S. Tuzi et al., manuscript in preparation).

order of 10^2 to 10^8 Hz (correlation time being in the order of 10^{-2} to 10^{-8} s), depending upon the portions from the transmembrane α-helices to surface residues including loops and N- or C-terminals under consideration, seems to be very important as compared with static pictures obtained so far by diffraction studies at cryo-temperature [3,7,25,26]. Under physiological conditions, however, such surface structure could be easily modified by a variety of environmental conditions such as ionic strength, temperature, pH, composition of lipids, etc., as determined by ^{13}C NMR studies on [3-^{13}C]Ala-labeled bR [32,38–41].

It is anticipated that the abovementioned dynamic picture of bR could be readily altered if 2D crystals were disrupted or partially disorganized due to failure of either proper formation of the trimeric structure or lattice assembly for the hexagonal crystals. Revealing the dynamic aspect of bR monomer under physiological conditions is, therefore, crucially important as a reference data in relation to better understanding of the biological significance of 2D crystals in bR. This data is also indispensable as background knowledge, giving rise to general ^{13}C NMR feature of monomeric proteins, because one may encounter with this situation as far as an attempt were made to incorporate an isolated membrane protein into lipid bilayers as proteoliposome. In other words, the availability of excellent, naturally occurring, stable 2D crystal as in the case of bR should be considered as a rather exceptional case. From these considerations, the following two choices are possible, either by reconstituted bR in DMPC bilayer, or several site-directed mutants to which key positions are modified to prevent formation of trimeric structure or lattice assembly.

Here, we utilize the latter approach to record the ^{13}C NMR spectra of [3-^{13}C]Ala-, [1-^{13}C]Ala- and Val-labeled W12L and W80L mutants (see Fig. 1 for amino acid sequence), in which side-chains of these two Trp residues are oriented outward from the transmembrane α-helices at the interface for lipid–protein interactions [6,25], and also bO from E1001 strain in which helix–helix interactions are modified due to lack of retinal [32], to search for the most appropriate ^{13}C-labeled amino acid residue to probe underlying conformational and dynamics changes. For this purpose, we have also examined Mn^{2+}-induced changes of ^{13}C NMR signals of wild-type to distinguish the signals of interfacial region between the surface loop and inner part of the transmembrane α-helices caused by their proximity to the surface bound Mn^{2+} ion as a relaxation agent.

It was found that the presence of disrupted or disorganized 2D lattice was clearly visualized by means of increased proportions of surrounding lipids per protein for these mutants and bO, respectively, together with broadened ^{13}C NMR signals from [3-^{13}C]Ala-labeled proteins due to acquired chain flexibility in the order of 10^{-4} s. Such dynamics change was more clearly noted as the completely suppressed ^{13}C NMR peaks from [1-^{13}C]Ala and Val-labeled proteins. It is also emphasized that distinct spectral change was noted for ^{13}C NMR spectra of [1-^{13}C]Ala- and Val-labeled wild-type, at the interfacial region of transmembrane α-helices between the surface loop and inner part by residue-specific manner. In the latter, the extent of suppressed ^{13}C NMR signals from such region is less pronounced due to altered correlation time longer than 10^{-4} s by more hindered rotational fluctuations in the presence of bulky side-chains at C_α moiety.

2. Materials and methods

[3-^{13}C]-L- and [1-^{13}C]-L-alanine (Ala) and [1-^{13}C]-L-valine (Val) were purchased from Cambridge Isotope Laboratories, Inc. (Andover, MA, USA) and used without further purification. W80L and W12L mutants were constructed by the method as described by Needleman et al. [42]. *H. salinarum* S9 and mutant strains, W80L, W12L, D85N and E1001 (wild-type but ret$^-$) were grown in the temporary synthetic (TS) medium [43], in which unlabeled L-Ala or L-Val were replaced by the ^{13}C-labeled ones. The purple membranes containing bR were isolated by a modified method of Oesterhelt and Stoeckenius [44] in which membrane samples were washed five times by centrifugation at 40,000 × *g* with 10 mM HEPES buffer to remove low-density fractions including red membranes and suspended in 5 mM HEPES buffer containing 0.02% NaN_3 and 10 mM NaCl at pH 7. Mn^{2+}-treatment of the purple membrane was carried out by resuspension of the membrane twice in 5 mM HEPES buffer (pH 7.0) containing 10 mM NaCl, 0.025% NaN_3 and 40 μM $MnCl_2$ to adjust final optical density of chromophores to 1.0. The samples thus prepared were concentrated by centrifugation and placed in a 5 mm o.d. zirconia pencil-type rotor for magic angle spinning. Samples were tightly sealed by Teflon caps and glued to the rotor by rapid Alardyte to prevent dehydration of pelleted samples through a pinhole in caps during magic angle spinning under a stream of dried compressed air.

^{13}C NMR measurements (100.6 MHz) were recorded in the dark at 20 °C on a Chemagnetics CMX-400 NMR spectrometer both by cross-polarization-magic angle spinning (CP-MAS) and single pulse, dipolar decoupled-magic angle spinning (DD-MAS) method, to distinguish ^{13}C NMR signals of more flexible membrane surface from those of more rigid transmembrane α-helices and loops [38,39]. The spectral width, contact time and acquisition times for CP-MAS experiments were 40 kHz, 1 and 50 ms, respectively. The 90° pulses for carbon and proton nuclei were 5 μs and the spinning rate was 2.6 and 4 kHz for [3-^{13}C]Ala- and [1-^{13}C]Ala- or Val-labeled proteins, respectively. Free induction decays were acquired with data points of 2 K. Fourier transform was carried out as 16 K points after 14 K points were zero-filled to improve digital spectral resolution. ^{13}C chemical shifts were initially referred to the carboxyl carbon signal of glycine (176.03 ppm from tetramethylsilane (TMS)) and converted to the value relative to TMS.

Absorption spectra were measured on a Shimadzu UV 2000 UV–Visible Spectrophotometer. Circular dichroism (CD) measurements were performed on an AVIV model 62DS using quartz cuvettes with path length of 0.01 cm under the concentration of 1 optical density.

3. Results

The visible absorption maximum of W12L and W80L was found to shift from 568 nm of wild-type to 562 and 556 nm by 6 and 12 nm, respectively. Further, the presence of bilobed feature in CD spectra [45,46] indicates that trimeric structure is preserved for W12L but is disrupted for W80L mutant (Fig. 2).

Fig. 3 illustrates the ^{13}C CP-MAS (left) and DD-MAS (right) NMR spectra of [3-^{13}C]Ala-labeled W80L (A and D) and W12L (B and E) mutants as compared with those of wild-type (C and F). It is noteworthy that the relative peak-intensities of lipids per the transmembrane α-helices of these mutants are increased appreciably with those of wild-type as judged from the intensity ratio of the surrounding lipid methyl group (marked by the asterisk) resonated at 19.0 ppm [47] to the peak of the protein resonated at 16.8 ppm (Ala 84 and 240, 244–246 at the C-terminal end, which is indifferent from the manner of crystalline packing mainly at the surface): they were estimated from the spectra in which the lipid methyl peak is not over-scaled, as 22 and 10 for W80L and W12L, respectively, with reference to 1 for wild-type. Further, the ^{13}C NMR peaks of the transmembrane α-helices for W12L and W80L mutants turned out to be substantially broadened as compared with those of wild-type, except for the peaks from the C-terminal residues protruding from the membrane surface, including the peaks at 15.8 and 16.8 ppm from the C-terminal end undergoing random fluctuation motions and Ala 228 and 233 from the C-terminal α-helix, respectively, connected to the transmembrane α-helix G [32,38,41] (see Fig. 1). In addition, several ^{13}C NMR peaks at 16.4–15.9 ppm from the transmembrane α-helices, including Ala 39, 53, 168 and 215 were preferentially suppressed [32,38,41] due to the presence of internal fluctuation with correlation time of 10^{-5} s interfered with the proton decoupling frequency of 50 kHz [49–51], caused by the fact that retinal–protein interactions are substantially modified as in the case of D85N mutant [48] or they are absent as in bO [32].

Fig. 4 illustrates the ^{13}C CP-MAS (left) and DD-MAS (right) NMR spectra of [1-^{13}C]Ala-labeled W80L (A and D) and W12L (B and E) mutants as compared with those of wild-type (C and F). Surprisingly, the ^{13}C CP-MAS NMR spectra of [1-^{13}C]Ala-labeled W80L and W12L mutants gave rise to featureless spectral patterns with appreciably reduced peak-intensities. This does not always means that

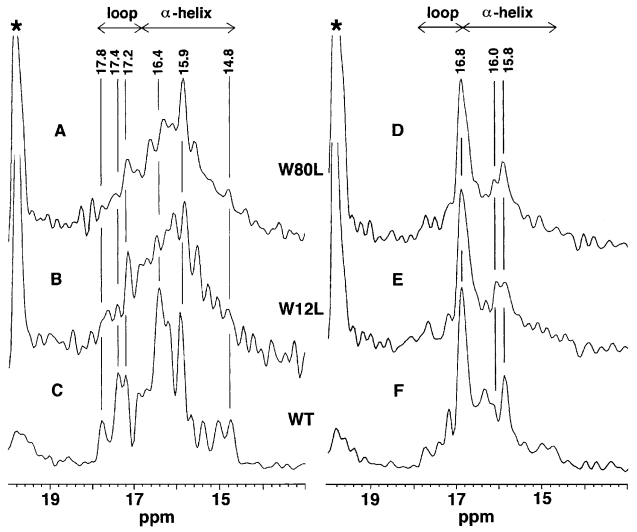

Fig. 3. ^{13}C CP-MAS (left) and DD-MAS (right) NMR spectra of [3-^{13}C]Ala-labeled W80L (A and D), W12L (B and E) and wild-type (C and F). The intense asterisked peak at 19.8 ppm for W80L and W12L was ascribed to the lipid methyl group [47].

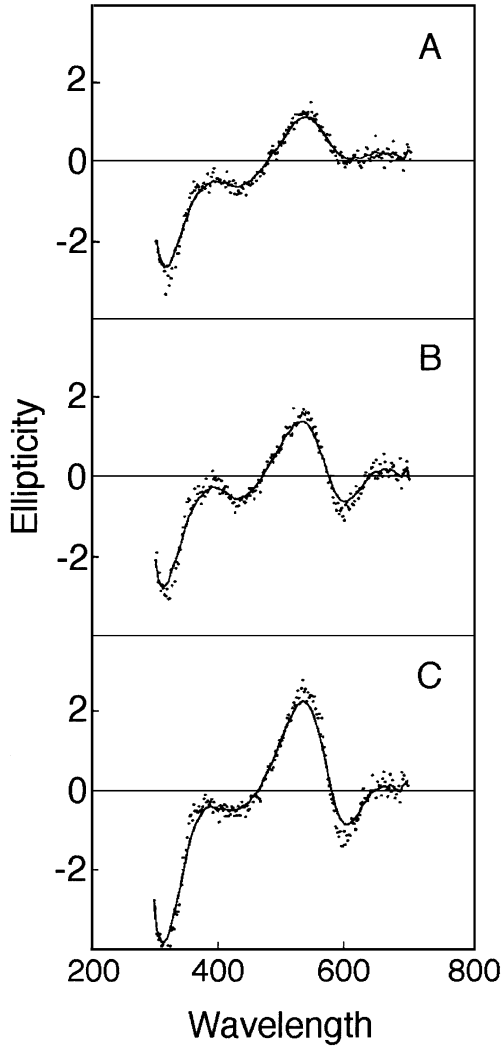

Fig. 2. CD spectra of W80L (A), W12L (B) and wild-type (C).

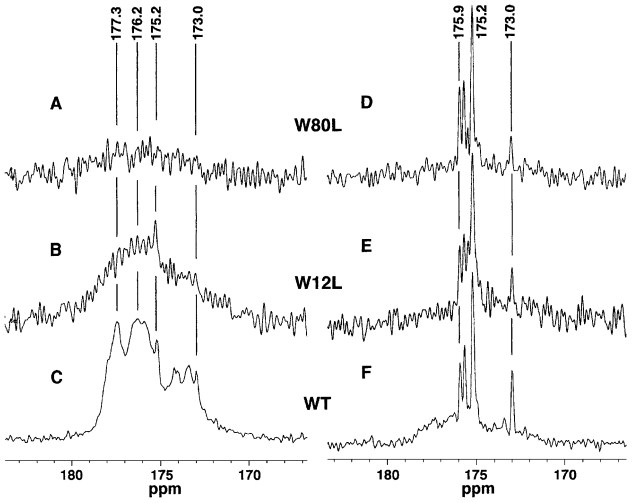

Fig. 4. ^{13}C CP-MAS (left) and DD-MAS (right) NMR spectra of [1-^{13}C]Ala-labeled W80L (A and D), W12L (B and E) and wild-type (C and F). The well-resolved ^{13}C NMR peaks from the DD-MAS NMR spectra resonated at 173.0–175.9 ppm were ascribed to the Ala residues located at the C- and N-terminal, including the C-terminal α-helix protruded from the surface, in spite of their peak region as interhelical loops [32].

these proteins exist as unfolded aggregates instead of properly folded state in view of the ^{13}C NMR spectra of [3-^{13}C]Ala-labeled proteins as illustrated in Fig. 3. Instead, the corresponding ^{13}C DD-MAS NMR spectra of these mutants (Fig. 4D and E) are very similar as compared with those of wild-type (Fig. 4F), indicating that their folding behavior is not unusual, at least as viewed from their surface structures. Therefore, the obviously distinct spectral features among the ^{13}C CP-MAS NMR spectra of [1-^{13}C]Ala-labeled W80L and W12L should be ascribed to failure of proper peak-narrowing process due to interference of incoherent frequency of conformational fluctuation in the transmembrane α-helices in these mutants in the order of 10^4 Hz (10^{-4} s) with coherent magic angle frequency [49–51].

At this point, it is crucially important to clarify whether the ^{13}C NMR signals so far recorded from the [1-^{13}C]Ala-labeled transmembrane α-helices of wild-type (Fig. 5D) are fully visible as in the case of [3-^{13}C]Ala-labeled bR [37] or not. This possibility should be always taken into account when one utilizes the former probe of larger chemical shift anisotropy as compared with that of the latter which is intrinsically very sensitive to the presence of fluctuation motions with time scale in the order of 10^{-4} s. Here, we compared the ^{13}C CP-MAS NMR spectra of [1-^{13}C]Ala-labeled D85N (Fig. 5A), bO from E1001 strain (Fig. 5B) and Mn^{2+}-treated bR (Fig. 5C) with those of wild-type (Fig. 5D), to clarify how the ^{13}C NMR signals of [1-^{13}C]Ala-labeled proteins could be altered by either modified helix–helix interactions or Mn^{2+}-induced spin relaxation rate. For this purpose, vertical scale of each traces was normalized with reference to the peak-intensities of the lowermost peak at 177.3 ppm, which turns out to be least susceptible to dynamics change because of the peak-assignment to residues located at the inner part, including Ala 53 (at 177.9 ppm) [52].

It is expected that such fluctuation-induced suppression of ^{13}C NMR signals from [1-^{13}C]Ala-bR could be recovered for bO or D85N mutant in which correlation times of the backbone fluctuations are already known to shift to the order of 10^{-5} s [32,48]. Obviously, such motions could be indifferent from the interference with magic angle spinning. Therefore, the enhanced peak-intensities of the ^{13}C CP-MAS NMR spectra of [1-^{13}C]Ala-labeled D85N (Fig. 5A) and bO (E1001) (Fig. 5B) were found at the transmembrane α-helical chains resonated at 176.5–175.8 ppm. This finding is consistent with our view that several ^{13}C NMR signals of [1-^{13}C]Ala-labeled wild-type might be also missing from the transmembrane α-helices, in addition to those of the loop region previously reported [40]. Further, we found that no ^{13}C NMR spectral change was noted for

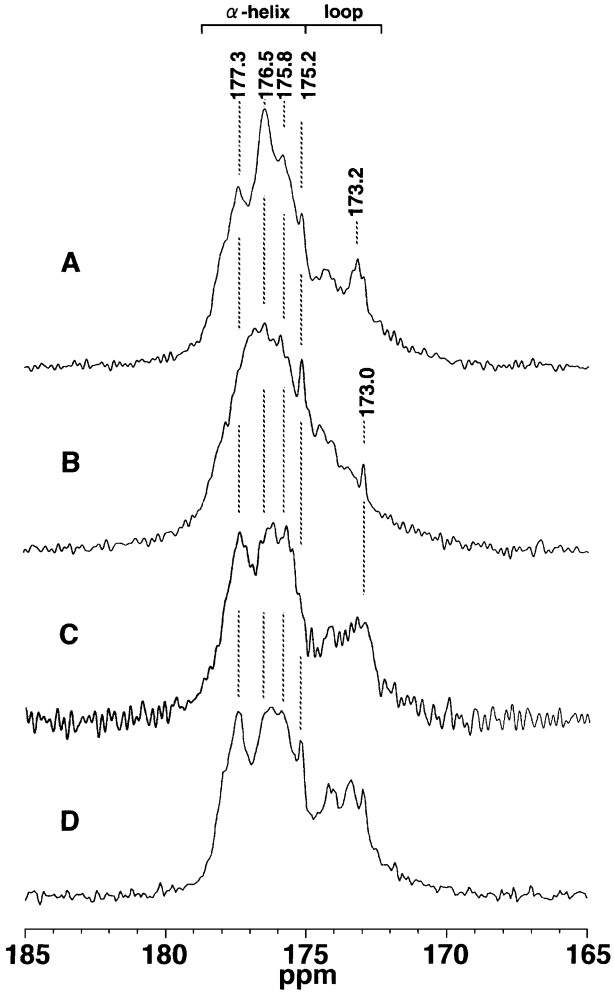

Fig. 5. ^{13}C CP-MAS NMR spectra of [1-^{13}C]Ala-labeled bR and its mutants. (A) D85N, (B) retinal-deficient E1001 strain, (C) wild-type in the presence of 40 μM M_nCl_2, and (D) wild-type. The peak at 173.0–173.2 ppm and 175.2 ppm are ascribed to the C-terminal α-helix protruded from the cytoplasmic surface (see Fig. 4D–F).

Mn^{2+}-treated [1-^{13}C]Ala-labeled wild-type (Fig. 5C), even if Mn^{2+} ion was added as a reagent for accelerated spin relaxation arising from the surface-bound Mn^{2+} ion [53,54] as compared with the ^{13}C NMR spectrum without Mn^{2+} ion (Fig. 5D). The absence of several minor peaks including 173.2 and 175.2 ppm can be ascribed to the C-terminal α-helix in the latter [39]. In fact, these ^{13}C NMR signals from the C-terminal α-helix protruding from the membrane surface were completely suppressed as more clearly viewed from the DD-MAS NMR spectra (spectrum not shown). Therefore, it is noteworthy that the ^{13}C CP-MAS NMR spectra of [1-^{13}C]Ala-labeled wild-type do not contain contributions from the residues located at the surfaces and interfacial regions of the transmembrane α-helices near at the membrane surface (up to 8.7 Å, estimated from the data of [3-^{13}C]Ala- [53] and [1-^{13}C]Pro-labeled bR (Tuzi et al., manuscript in preparation; indicated by the horizontal dotted lines in Fig. 1) at ambient temperature [53].

In contrast, it appears that the ^{13}C NMR spectral feature of the interfacial regions from [1-^{13}C]Val-bR is not always the same as that of [1-^{13}C]Ala-bR described above: the well-resolved ^{13}C NMR spectra (Fig. 6A) were obtained for the former, as compared with those of the latter (Fig. 5D). To locate Mn^{2+}-ion-induced suppression of ^{13}C NMR peaks, we compared the ^{13}C NMR spectra of [1-^{13}C]Val-bR without (Fig. 6A) and with Mn^{2+} ion (Fig. 6B). Interestingly, the peak-intensities of at least four signals were appreciably suppressed by accelerated spin–spin relaxation rate in the presence of Mn^{2+} ion [53,54]: 174.6, 174.0, 172.9 (Val 69) and 171.1 ppm (Val 199). The latter two signals from these loops are naturally suppressed due to the proximity of the preferred binding site of Mn^{2+} ion at the extracellular surface [55]. In contrast to the case of [1-^{13}C]Ala-bR, the ^{13}C NMR signals of [1-^{13}C]Val-bR from both such loops and interfacial regions in the transmembrane α-helices are not always suppressed by interference of undergoing fluctuation motions with magic angle spinning alone. This is because fluctuation frequencies about the torsion angles of amino acid residues with bulky side-chains at C_α moiety such as Val could be shifted to low frequency than 10^4 Hz and indifferent from such fluctuation-induced suppression of peaks (Fig. 6). Therefore, the former two peaks of Fig. 5A are obviously from Val residues located near at the membrane surface, although ^{13}C NMR signal from Val 179 and 187 is superimposed upon the peak from residues near at the membrane surface at 174.60 ppm (Kira et al., manuscript in preparation).

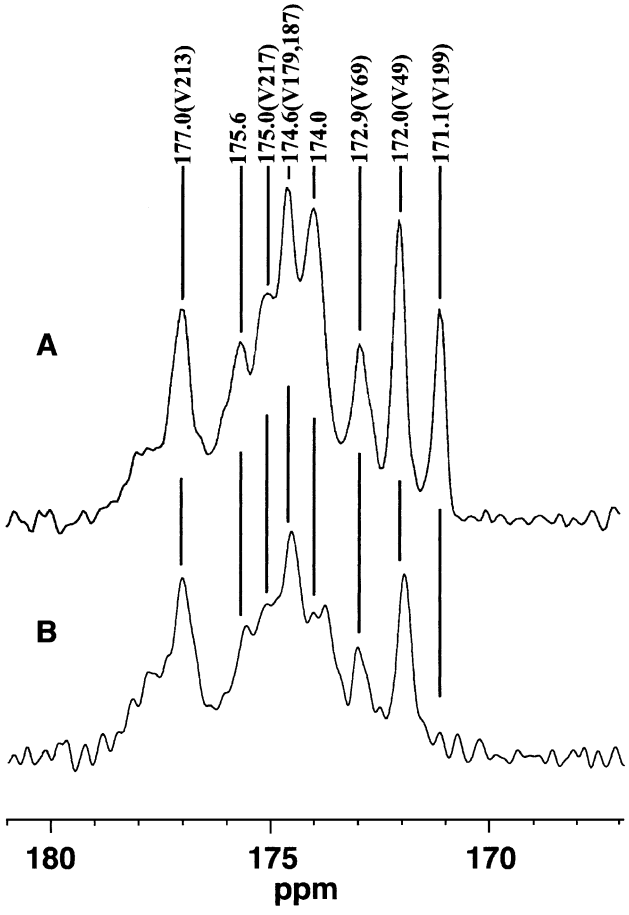

Fig. 6. ^{13}C CP-MAS NMR spectra of [1-^{13}C]Val-labeled bR without (A) and with treatment of 40 μM M_nCl_2 (B).

To further clarify the differential behavior of ^{13}C NMR spectra from [1-^{13}C]Val and Ala probes, we compared the ^{13}C CP-MAS (left) and DD-MAS (right) NMR spectra of [1-^{13}C]Val-labeled bO from E1001 (Fig. 7A and E), W80L (Fig. 7B and F), W12L (Fig. 7C and G). In contrast to the case of [1-^{13}C]Ala-labeled bR (Fig. 4A and D), all the ^{13}C NMR signals which resonated at a peak-position higher than 173.5 ppm should be ascribed to the residues located at the interhelical loops (172.9 and 171.0 ppm), although the ^{13}C NMR peak from Val 49 (172.0 ppm) of the transmembrane α-helix resonated at the loop region due to the presence of Val–Pro sequence [56]. As a result, it was found that the two ^{13}C DD-MAS NMR peaks (171.0 and 172.9 ppm) of Val 69 (B–C loop) and 199 (F–G loop) for E1001 strain, W80L and W12L were motionally suppressed due to acquisition of fluctuation frequency in the order of 10^4 Hz (Fig. 7E–G). Naturally, these two peaks are suppressed (or decreased) by the addition of Mn^{2+} ion in view of the ^{13}C NMR signals from the residues in the membrane surface (Fig. 6B). Further, the manner of the peak-suppression for the transmembrane α-helices for W80L and W12L mutants, as detected by the ^{13}C CP-MAS NMR spectra, is very similar to that of [1-^{13}C]Ala-bR, as described above (Fig. 4). It is also interesting to note that the ^{13}C peak-intensities of [1-^{13}C]Val-labeled bO from E1001 are substantially broadened and suppressed with reference to those of wild-type, in contrast to the increased peak-intensities for [1-^{13}C]Ala-labeled E1001 protein as observed in Fig. 5B. Again, this is caused by the differential response to the motional frequencies between Ala and Val residues, as mentioned above.

4. Discussion

4.1. Tertiary structure changes either by modified lipid–helix or helix–helix interactions induced by site-directed mutation, removal or addition of retinal

First of all, it is demonstrated, on the basis of the CD measurements (Fig. 2) that the trimeric complex is no longer stable in W80L but still present in W12L mutant, although a possibility of "a mixture of crystalline and non-crystalline components" cannot be completely excluded in view of the manner of sample preparation. In any case, the Trp residues under consideration in these mutants are located at the key positions responsible for suitable lipid–helix interactions in view of the 3D structure of bR revealed by X-ray diffraction [4–6]. In spite of such distinct changes for the trimer formation, the ^{13}C NMR spectral features of [3-^{13}C]Ala-labeled W12L and W80L are very similar: individual ^{13}C NMR signals of both mutants are substantially broadened as compared with those of wild-type, together with substantially reduced peak-intensities (Fig. 3). Besides, the estimated number of surrounding lipids is roughly determined by the relative lipid-to-protein intensity ratio previously described as 220 and 100 for W80L and W12L, respectively, with reference to that of wild-type, taken as 10 [3], provided that scrambling to the lipids from incorporated [3-^{13}C]Ala-label is not changed between wild-type and these mutants. It appears that this estimate seems to be reasonable because bR monomer is embedded in the "sea" of lipids, together with boundary lipids in direct contact with bR. In fact, it was previously shown, on the basis of an ESR study of spin-labeled phospholipids and freeze-fracture electron microscopy, that monomeric bR is associated with 18–21 boundary lipids at temperatures above the gel to liquid crystalline temperature of synthetic lipid bilayer [57]. In particular, several ^{13}C NMR peaks from the transmembrane α-helices, including Ala 39 (helix B), 53 (helix B), 168 (helix F) and 215 (helix G) were preferentially suppressed in these W80L and W12L mutants as recorded by both CP-MAS and DD-MAS methods. This means that modified lipid–helix interactions caused by replacement of Trp 12 (helix A) and 80 (helix C) with Leu induced fluctuation motions with frequency in the order of 10^5 Hz at the transmembrane α-helices (B, F and G helices) which are interfered with the proton decoupling frequency.

In contrast, the ^{13}C CP-MAS NMR spectra of [1-^{13}C]Ala and Val-labeled W12L and W80L mutants were almost completely suppressed (the left traces in Figs. 4 and 7). Further, the ^{13}C CP-MAS NMR spectrum of [1-^{13}C]Val-labeled bO from retinal-deficient E1001 strain (Fig. 7A (left)) was substantially broadened with suppressed peak-intensities as compared with that prepared from bR by removal of retinal as reported previously [32]. Obviously, this is caused by acquired flexibility of the protein backbone as a result of disrupted trimeric complex and subsequent hexagonal assembly without retinal. As pointed out previously, however, the tertiary structure of bO in the hexagonal array seems to be retained even after retinal was removed from bR in the purple membrane in which once the tertiary structure is formed [32]. In other words, an irreversible conformational change was induced during bR regeneration from bO arising from retinal-deficient strain, because retinal is essential as template for complete folding [32]. These findings indicate that the ^{13}C NMR spectral features of ^{13}C-labeled bR, its mutants and bO are substantially varied together with the disrupted or disorganized hexagonal packing, rather than the presence or absence of the trimeric complex as judged from the CD spectra (Fig. 2). Therefore, the observed spectral feature depends mainly on the tertiary structure in hexagonally packed 2D lattice of purple membrane rather than that of the monomeric unit.

Structural determinants of purple membrane as one of the best models for membrane proteins constituting 2D crystals have been extensively examined in terms of helix–helix and lipid–helix interactions as essential factors by means of structural, calorimetric and reconstitution studies using wild-type and site-directed mutants [21,28,32–34]. In this context, the significance of the present data as to W12L and W80L mutants examined here is undoubtedly related with potential role of such bulky side-chains in Trp 12 and 80 in lipid–protein interactions leading to stabilization of the hexagonal assembly of bR. In fact, Besir and Oesterhelt showed that bR trimer is disrupted by substitution of Trp 80 with smaller amino acid residues (cited in Ref. [23]). It was further found in this paper that the hexagonal lattice regulates the dynamic aspect of individual helices, restraining molecular fluctuation of the transmembrane helices from 10^4 Hz of proteins from disrupted or disorganized lattice to 10^2 Hz in the crystalline lattice consisting of the trimeric structures. In this connection, it is interesting to note that interaction of sulfoglycolipid, 3-sulfate-Gal*p*β1–6Man*p*α1–2Glc*p*α-1-archaeol (S-TGA-1) in the trimer interior and Trp 80 is crucial for lattice assembly [23]. For this reason, it is emphasized from ^{13}C NMR spectral point of view that lattice formation is essential as one of constraints to reduce motional fluctuations in the transmembrane α-helices in membrane proteins.

It is interesting to note that the visible absorption maxima of W12L (562 nm) and W80L (556 nm) are very close to those of bR in the presence of detergent molecules, DOC (562 nm) and CHAPS/DM (558 nm), respectively, to cause delipidation [58]. Obviously, this finding is consistent with the view that replacement of Trp at 12 and 80 of bR with Leu residues results in deletion of specific lipid–protein interaction in these positions, because the total number of bound lipids per intact bR was reduced upon delipidation from 10 in wild-type to six and three to four after treatments with DOC [28] and CHAPS [59], respectively. In addition, solubilization of bR by a variety of detergents such as DM, TX-100, TN-101 and SDS results in further changes in the absorption maximum to 550–437 nm [59]. Accordingly, it is well-recognized that acquired space to allow helix motion

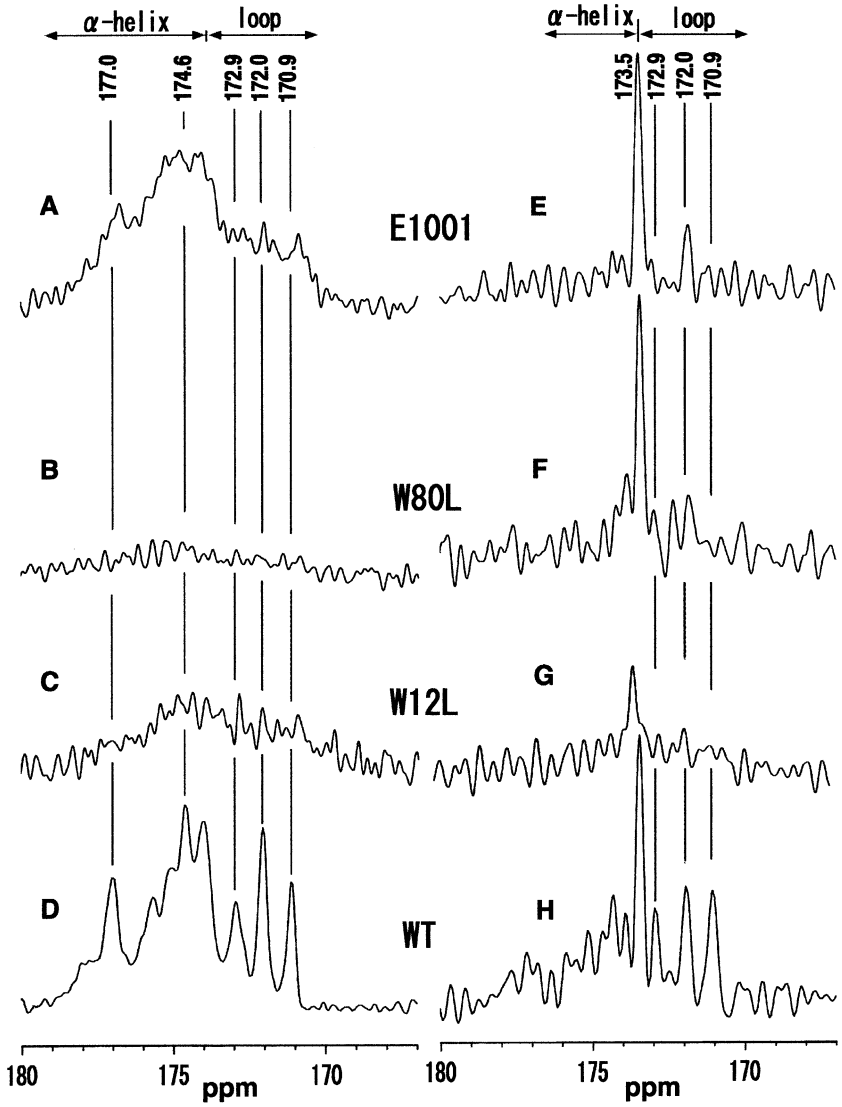

Fig. 7. ^{13}C CP-MAS (left) and DD-MAS (right) NMR spectra of [1-^{13}C]Val-labeled wild-type, W12L, W80L and E1002 strain (from the bottom to top traces).

caused by such modified lipid–protein interactions results in modified retinal–helix interactions, as seen by the changes in the absorption maximum. Conceivably, it appears that these absorption changes are not always sensitive to the presence or absence of crystalline lattice, although further conformational changes accompanied by solubilization resulted in further shifts in the absorption maxima.

4.2. Residue-specific fluctuation frequencies in the transmembrane α-helices in relation to the search for the most appropriate ^{13}C NMR probes

The present ^{13}C NMR approach has proved to be an excellent means to examine a plausible fluctuation of millisecond to microsecond (10^{-4} to 10^{-5} s), in the transmembrane α-helices and loops of wild-type and site-directed mutants, as viewed from fluctuation-induced suppression of peaks at ambient temperature [38–41]. In particular, ^{13}C NMR peaks of interhelical loops in [1-^{13}C] and [2-^{13}C]Ala-bR and mutants were completely suppressed due to such fluctuation motions arising from the least number of constraints from inter-residual hydrogen bonds to prevent such motions. On the contrary, ^{13}C NMR signal of [1-^{13}C]Val-labeled residues 69 and 199 are clearly visible in spite of their location at the B–C and F–G loops, respectively. Consequently, it is notable that ^{13}C NMR signals from the loop regions are made visible as viewed from [1-^{13}C]Val-labeled 199, but not from [1-^{13}C]Ala-labeled 196 [40], even though both residues are located at the same F–G loop but only two residues apart. This finding indicates that undergoing fluctuation frequency is not only dependent upon the local conformation but also on the particular amino acid residues involved. Nevertheless, it is also taken into account that the ^{13}C NMR signals of [1-^{13}C]Val-labeled 69 and 199 are

suppressed for E1001, W80L and W12L by acquisition of fluctuation motion due to either disrupted or disorganized crystalline lattice (Fig. 7E–G).

In addition, any amino acid residues of transmembrane α-helices neighbored with such loop region could acquire similar flexibility, also depending upon the distance from the membrane surface [40]. This is the reason why detailed analysis of ^{13}C NMR behavior from residues located at the interfacial region is very important. In this connection, it is noted that the ^{13}C NMR behavior of the transmembrane α-helices from the residues located at the interfacial region seems to be again not the same between Ala and Val probes. In fact, amplitude and/or frequency of such fluctuation motions, if any, are not always the same between the two types of residues, even if these two types of residues are located at the same domain. As a convenient means to locate the ^{13}C NMR signals from the interfacial residues, we can roughly distinguish the ^{13}C NMR signals of any given amino acid residues located at the interfacial regions from the remaining inner part of the transmembrane α-helices, on the basis of Mn^{2+}-ion-induced suppression of peaks [53,54], demonstrated in Figs. 5 and 6. As previously described, it is noteworthy that ^{13}C NMR signals of [1-^{13}C]Ala-bR from the interfacial region are almost completely suppressed, although the corresponding peaks of [1-^{13}C]Val-bR are fully visible. Such distinction is very important to choose the most suitable intrinsic probe molecules to examine conformation and dynamics of membrane proteins in general.

In general, 3D structure and dynamics of a single polypeptide chain can be represented by specifying the following three sets of angles ω_i, ϕ_i, and φ_i, which define the torsion angles around the bonds C′ (C=O)−N, N−C_α, C_α−C′ (=O) in residue i and their time-dependent variations, respectively. This problem is further reduced to the assignment of the latter two angles in the peptide backbone and the orientation of the side-chain, because the angle ω_i is, in many instances, fixed to 180° taking into account the rigid peptide plane. Conformational fluctuations in the transmembrane α helices, for instance, can be expressed by time-dependent deviations from the angles corresponding to the lowest energy minima (ϕ_i, φ_i)=(−57°, −47°) in the conformation map [60]. This minimum is shallow for the Gly–Gly sequence in view of widely allowed space but is changed to limited area together with the presence of bulky side-chain in C_α as inferred from the map of Gly–Ala sequence [60]. As a result, it is expected that such fluctuation may be hindered in the presence of more bulky side-chain at the C_α position as in Val residue. It appears that this happens as residue-specific acquisition of local fluctuation motions: there appears a distinct change in the ^{13}C NMR behavior between Ala and Val residues in response to such low-frequency fluctuations, as manifested by the ^{13}C NMR spectra of [1-^{13}C]Ala- and Val-labeled bR and its mutants (Figs. 5 and 6). Even in crystalline peptides, it is noteworthy that low-amplitude libration motion, consisting of fluctuation in the peptide plane about the $C_\alpha C_{\alpha'}$ axis for Gly–Gly sequence, is seen in the crystalline peptides with time scale of 10^{-4} s [61].

It should be taken into account that such fluctuation motions, if any, should be accompanied by instantaneous deformation of α-helical structures involving distortion or breakage of a number of inter-residual N−H...O=C hydrogen bonds. Nevertheless, it should be recognized that the α-helical structure is not always considered as a rigid rod but rather flexible with fluctuation motions in the time scale of 10^{-4} to 10^{-5} s, as mentioned above. We have previously showed that N−H moiety acting as proton donor in hydrogen bonds undergoes perpendicular thermal fluctuations with respect to the direction of N...O vector as found for elongated N−H distance, determined as measured by analysis of dipolar interaction [61] as well as $^{15}N...O=^{13}C$ distances measured by rotational echo double resonance (REDOR) as compared with those by neutron or X-ray diffraction studies [62,63].

In spite of the presence of such fluctuation motions in the monomeric or trimeric complexes as demonstrated above, ^{13}C NMR signals of [3-^{13}C]Ala-labeled proteins can be used as the most appropriate intrinsic probes to examine the general conformational feature of membrane proteins, as viewed from their short spin-lattice relaxation times, least possibility of scrambling and accidentally overlapped signals with those of other residues, and the minimum expenditure for experiments. It should be taken into account that ^{13}C NMR signals from this probe are suppressed if specific domains acquire flexibility of motions with frequency of 10^5 Hz occurring for certain mutants. In such cases, it is advised to utilize either [1-^{13}C]Ala or Val-probes instead, although the latter is more favorable in view of the availability of signals for interfacial region between the surface and inner part of the transmembrane α-helices.

Acknowledgements

This work was supported, in part, by a Grant-in-Aid for Scientific Research from the Ministry of Education, Science, Culture and Sports of Japan and Shorai Foundation for Science and Technology.

References

[1] B.J. Bormann, D.M. Engelman, Annu. Rev. Biophys. Biomol. Struct. 21 (1992) 223–242.
[2] M.H.B. Sowell, D.C. Rees, Adv. Protein Chem. 46 (1995) 279–311.
[3] N. Grigorieff, T.A. Ceska, K.H. Dowing, J.M. Baldwin, R. Henderson, J. Mol. Biol. 259 (1996) 393–421.
[4] E. Pebay-Peyroula, G. Rummel, J.P. Rosenbusch, E.M. Landau, Science 277 (1997) 1676–1681.
[5] H. Lucke, H.T. Richter, J.K. Lanyi, Science 280 (1998) 1934–1937.
[6] L. Essen, R. Siegert, W.D. Lehmann, D. Oesterhelt, Proc. Natl. Acad. Sci. U. S. A. 95 (1998) 11673–11678.

[7] H. Sato, K. Takeda, K. Tani, T. Hino, T. Okada, M. Nakasako, N. Kamiya, T. Kouyama, Acta Crystallogr., D 55 (1999) 1251–1256.
[8] W.A. Havelka, R. Henderson, J.A. Heymann, D. Oesterhelt, J. Mol. Biol. 234 (1993) 837–846.
[9] M. Kolbe, H. Besir, L.-O. Essen, D. Oesterhelt, Science 288 (2000) 1390–1396.
[10] E.R.S. Kunji, E.N. Spudich, R. Grisshammer, R. Henderson, J.L. Spudich, J. Mol. Bio. 308 (2001) 279–293.
[11] H. Luecke, B. Schobert, J.K. Lanyi, E.N. Spudich, J.L. Spudich, Science 293 (2001) 1499–1503.
[12] A. Royant, R.A. Nollert, P. Edman, R. Neutze, E.M. Landau, E. Pebay-Peyroula, J. Navaro, Proc. Natl. Acad. Sci. U. S. A. 28 (2001) 10131–10136.
[13] J. Deisenhofer, O. Epp, K. Miki, R. Huber, H. Michel, Nature 318 (1985) 618–624.
[14] W. Kuhlbrandt, D.N. Wang, Y. Fujiyoshi, Nature 367 (1994) 614–621.
[15] G. McDermott, S.M. Prince, A.A. Freer, A.M. Hawthornthwaite-Lawless, M.Z. Papiz, R.J. Cogdell, N.W. Isaacs, Nature 374 (1995) 517–521.
[16] S. Iwata, C. Ostermeier, B. Ludwig, H. Michel, Nature 376 (1995) 660–669.
[17] T. Tsukihara, H. Aoyama, E. Yamashita, T. Tomizaki, H. Yamaguchi, K. Shinzawa-Itoh, R. Nakashima, R. Yano, S. Yoshikawa, Science 272 (1996) 1136–1144.
[18] D.A. Doyle, J.M. Cabral, R.A. Pfuetzner, A. Kuo, J.M. Gulbiss, S.L. Cohen, B.T. Chait, R. MacKinnon, Science 280 (1998) 69–77.
[19] G. Chang, R.H. Spencer, A.T. Lee, M.T. Barclay, D.C. Rees, Science 282 (1998) 2220–2226.
[20] K.S. Huang, H. Bayleyn, M.J. Liao, E. London, H.G. Khorana, J. Biol. Chem. 256 (1981) 3802–3809.
[21] A.E. Blaurock, W. Stoekenius, Nature, New Biol. 233 (1971) 152–155.
[22] D. Oesterhelt, Curr. Opin. Struct. Biol. 8 (1998) 489–500.
[23] M.P. Krebs, T.A. Isenbarger, Biochim. Biophys. Acta 1460 (2000) 15–26.
[24] T. Haltia, E. Freire, Biochim. Biophys. Acta 1228 (1995) 1–27.
[25] H. Luecke, B. Schobert, H.T. Richter, J.P. Cartaille, J.K. Lanyi, J. Mol. Biol. 291 (1999) 899–911.
[26] H. Belrhali, P. Nollert, A. Royant, C. Menzel, J.P. Rosenbusch, E.M. Landau, E. Pebay-Peyroula, Structure 7 (1999) 909–917.
[27] M. Kates, N. Moldoveanu, L.C. Stewart, Biochim. Biophys. Acta 1169 (1993) 46–53.
[28] N. Grigorieff, E. Beckmann, F. Zelmlin, 254 (1995) 404–415; 91 (1994) 11854–11858.
[29] B. Sternberg, C. L'Hostis, C.A. Whiteway, A. Watts, Biochim. Biophys. Acta 1108 (1992) 21–30.
[30] Y. Mukohata, Y. Sugiyama, Y. Kaji, J. Usukura, E. Yamda, Photochem. Photobiol. 33 (1981) 593–600.
[31] J. Usukura, E. Yamada, Y. Mukohata, Photochem. Photobiol. 33 (1981) 475–481.
[32] S. Yamaguchi, S. Tuzi, M. Tanio, A. Naito, J.K. Lanyi, R. Needleman, H. Saitô, J. Biochem. (Tokyo) 127 (2000) 861–869.
[33] M.P. Krebs, W. Li, T.P. Halmbeck, J. Mol. Biol. 267 (1997) 172–183.
[34] T.A. Isenbarger, M.P. Krebs, Biochemistry 38 (1999) 9023–9030.
[35] T.A. Isenbarger, M.P. Krebs, Biochemistry 40 (2001) 11923–11931.
[36] J. Cladera, J. Torres, E. Padros, Biophys. J. 70 (1996) 2882–2887.
[37] S. Tuzi, S. Yamaguchi, A. Naito, R. Needleman, J.K. Lanyi, H. Saitô, Biochemistry 35 (1996) 7520–7527.
[38] H. Saitô, S. Tuzi, S. Yamaguchi, M. Tanio, A. Naito, Biochim. Biophys. Acta 1460 (2000) 39–48.
[39] H. Saitô, S. Tuzi, M. Tanio, A. Naito, Annu. Rep. NMR Spectrosc. 47 (2002) 39–108.
[40] S. Yamaguchi, S. Tuzi, K. Yonebayashi, A. Naito, R. Needleman, J.K. Lanyi, H. Saitô, J. Biochem. (Tokyo) 129 (2001) 373–382.
[41] S. Yamaguchi, K. Yonebayashi, H. Konishi, S. Tuzi, A. Naito, J.K. Lanyi, R. Needleman, H. Saitô, Eur. J. Biochem. 268 (2001) 2218–2228.
[42] R. Needleman, M. Chang, B. Ni, G. Varo, J. Fornes, S.H. White, J.K. Lanyi, J. Biol. Chem. 266 (1991) 11478–11484.
[43] H. Onishi, M.E. McCance, N.E. Gibbons, Can. J. Microbiol. (1965) 365–373.
[44] D. Oesterhelt, W. Stoeckenius, Methods Enzymol. 31 (1974) 667–678.
[45] M.P. Heyn, P.-J. Bauer, N.A. Dencher, Biochem. Biophys. Res. Commun. 67 (1975) 897–903.
[46] T.G. Ebrey, B. Becher, B. Mao, P. Kilbride, J. Mol. Biol. 112 (1977) 377–397.
[47] S. Tuzi, A. Naito, H. Saitô, Eur. J. Biochem. 239 (1996) 294–301.
[48] Y. Kawase, M. Tanio, A. Kira, S. Yamaguchi, S. Tuzi, A. Naito, M. Kataoka, J.K. Lanyi, R. Needleman, H. Saitô, Biochemistry 39 (2000) 14472–14480.
[49] W.P. Rothwell, J.S. Waugh, J. Chem. Phys. 74 (1981) 2721–2732.
[50] D. Suwelack, W.P. Rothwell, J.S. Waugh, J. Chem. Phys. 73 (1980) 2559–2569.
[51] A. Naito, A. Fukutani, M. Uitdehaag, S. Tuzi, H. Saitô, J. Mol. Struct. 441 (1998) 231–241.
[52] S. Yamaguchi, S. Tuzi, T. Seki, M. Tanio, R. Needleman, J.K. Lanyi, A. Naito, H. Saitô, J. Biochem. (Tokyo) 123 (1998) 78–86.
[53] S. Tuzi, J. Hasegawa, R. Kawaminami, A. Naito, H. Saitô, Biophys. J. 81 (2001) 425–434.
[54] I. Solomon, Phys. Rev. 99 (1955) 559–565.
[55] S. Tuzi, S. Yamaguchi, M. Tanio, H. Konishi, S. Inoue, A. Naito, R. Needleman, J.K. Lanyi, H. Saitô, Biophys. J. 76 (1999) 1523–1531.
[56] M. Tanio, S. Inoue, K. Yokota, T. Seki, S. Tuzi, R. Needleman, J.K. Lanyi, A. Naito, H. Saitô, Biophys. J. 77 (1999) 431–442.
[57] P. Gale, Biochem. Biophys. Res. Commun. 196 (1993) 879–884.
[58] M. Tanio, S. Tuzi, S. Yamaguchi, H. Konishi, A. Naito, R. Lanyi, J.K. Lanyi, H. Saitô, Biochim. Biophys. Acta 1375 (1998) 84–92.
[59] M. Seigneuret, J.-M. Neumann, J.-L. Rigaud, J. Biol. Chem. 266 (1991) 10066–10069.
[60] G.N. Ramachandran, V. Sasisekharan, Adv. Protein Chem. 23 (1968) 283.
[61] A. Fukutani, A. Naito, S. Tuzi, H. Saitô, J. Mol. Struct. 602–603 (2002) 491–503.
[62] S. Kimura, A. Naito, S. Tuzi, H. Saitô, J. Mol. Struct. 602–603 (2002).
[63] S. Kimura, A. Naito, H.H. Saitô, K. Ogawa, A. Shoji, J. Mol. Struct. 562 (2001) 197–203.